Drug and Alcohol Dependence 263 (2024) 112416

Contents lists available at ScienceDirect

Drug and Alcohol Dependence

journal homepage: www.elsevier.com/locate/drugalcdep

Hub disruption in HIV disease and cocaine use: A connectomics analysis of brain function

Kareem Al-Khalil [a,*], Ryan P. Bell [a,d], Sheri L. Towe [a,d], Jessica R. Cohen [b], Syam Gadde [c], James Mu [a], Shana A. Hall [a], Christina S. Meade [a,c,d]

[a] Duke University School of Medicine, Department of Psychiatry and Behavioral Sciences, 2400 Pratt Street, Durham, NC 27705, USA
[b] University of North Carolina at Chapel Hill, Department of Psychology and Neuroscience, 100 E. Franklin Street Suite 200, Chapel Hill, NC 27599, USA
[c] Duke University Medical Center, Brain Imaging Analysis Center, 40 Duke Medicine Cir #414, Durham, NC 27710, USA
[d] Wake Forest University, School of Medicine, 475 Vine Street, Winston-Salem, NC 27101, USA

ARTICLE INFO

Keywords:
Hub disruption index
HIV disease
Cocaine use
Centrality
Connectomics

ABSTRACT

Background: Cocaine use (CU) is prevalent in people with HIV (PWH). Both conditions are linked to changes in cognitive functioning and neural network topology. The current study utilizes graph theory to investigate functional connectomics associated with HIV and CU, focusing on disruption of densely connected nodes called hubs.

Methods: Resting state functional magnetic resonance imaging (fMRI) from 206 adults (ages 22–55 years) were analyzed. A HIV x CU factorial design was implemented with participants in four groups: HIV+CU (n= 41), HIV only (n= 88), CU only (n= 36), and controls (n= 41). Functional connectomes were constructed, and thresholded graph metrics were calculated. Network centrality metrics – betweenness centrality (BC), participation coefficient (PC), and within module degree (WD) – were quantified into hub disruption indices (HDI). For each index, a 2×2 ANCOVA was performed controlling for education.

Results: Participants were 68 % male and 74 % African-American with a mean age of 44.4 years. HIV and CU were associated with hub disruption in all three indices. Interactions were significant for HDI-PC and HDI-WD, such that HIV disease was associated with greater hub disruption among participants without CU, but not among participants with CU. Overall, lower global cognitive functioning was associated with greater hub disruption on all three indices.

Conclusions: Widespread hub disruption was evident in HIV disease and CU, highlighting topological reorganization in both diseases with neurocognitive effects. Hub-related measures inform functional connectivity disruptions in HIV disease and CU, particularly with respect to changes in network topology throughout the connectome.

1. Introduction

An estimated 30–50 % of people with HIV (PWH) exhibit cognitive impairment (Cysique et al., 2014a, 2004b; Heaton et al., 2010; Wang et al., 2020) that impacts day-to-day functioning (Anand et al., 2010; Cattie et al., 2012; Heaton et al., 2004; Laverick et al., 2017; Shrestha and Copenhaver, 2016; Thames et al., 2013). Underlying HIV-related cognitive impairment are systematic disruptions in brain physiology and functioning (Ances and Ellis, 2007; Sanmarti et al., 2014), including functional connectivity (FC) changes in multiple cortical and subcortical networks (du Plessis et al., 2015; Egbert et al., 2018; Plessis et al., 2017; Wang et al., 2011). The effects of HIV neuropathogenesis are further exacerbated by cocaine use (CU) (Cai et al., 2016; Chilunda et al., 2019), which is disproportionately prevalent in PWH compared to people without HIV (Shiau et al., 2017). Given that CU also causes persistent neurobiological changes in many neural networks affected by HIV disease (Adinoff et al., 2015; Cisler et al., 2013; Feil et al., 2010; Geng et al., 2017; Ma et al., 2015), research is needed to delineate the independent and additive effects of these two conditions on neural networking.

Brain connectomics can be used to identify large-scale changes in

* Corresponding author.
E-mail addresses: kalkhal@gmail.com (K. Al-Khalil), rpbell@wakehealth.edu (R.P. Bell), stowe@wakehealth.edu (S.L. Towe), jrcohen@unc.edu (J.R. Cohen), syam.gadde@duke.edu (S. Gadde), james.mu@duke.edu (J. Mu), shana@limbix.com (S.A. Hall), cmeade@wakehealth.edu (C.S. Meade).

https://doi.org/10.1016/j.drugalcdep.2024.112416
Received 5 January 2024; Received in revised form 8 July 2024; Accepted 7 August 2024
Available online 21 August 2024

brain connectivity in PWH (Abidin et al., 2018; Hall et al., 2021; Zhuang et al., 2021) and CU (Liang et al., 2015; Orsini et al., 2018). In a connectomics framework, the brain is conceptualized as an interactive system of regions, or nodes. Graph theoretical analysis utilizes mathematical modeling of connections between nodes, termed edges, to provide topological information about brain networks (Bullmore and Bassett, 2011; Bullmore and Sporns, 2009; Rubinov and Sporns, 2010; Sporns, 2018). Further, functional Magnetic Resonance Imaging (fMRI) data can be used to construct functional connectomes, with edges representing pairwise co-variances between the activation time-series of nodes. Graph theory has been used to ascertain properties of modularity in neural networks. Modularity refers to the decomposition of neural connections into networks, or modules, with nodes within each network being more densely interconnected to each other compared to nodes of other networks. Network integration characterizes communication between functional networks, and network segregation refers to functional independence of individual networks. Some studies using graph theory metrics found connectivity deficits in HIV disease (Zhuang et al., 2021), but other studies showed no effects of HIV disease with the same graph metrics (Abidin et al., 2018). Other research has found greater global efficiency in PWH compared to sero-negative controls (Hall et al., 2021; Minosse et al., 2020). Meanwhile, studies have associated CU with greater clustering in reward networks (Orsini et al., 2018), but reduced inter-module connectivity (Liang et al., 2015). Although graph theory studies examining the effects of CU are rare, methamphetamine use has been linked with greater efficiency and lower clustering throughout executive, default mode, salience, limbic, and cerebellar networks (Li et al., 2023; Li et al., 2022; Mansoory et al., 2022). While these studies may inform stimulant related topological effects, research findings from studies using graph theory in CU and HIV disease lack consensus. Certainly, sample heterogeneity in multiple variables, such as poly-substance use, disease severity, and treatment status, contribute to inconsistent findings across studies (Zenebe et al., 2021). Other possible contributions involve differences in analytical techniques (Bowring et al., 2019; Bowring et al., 2022; Wei et al., 2022).

Some of the limitations of graph theory could be circumvented by focusing on centrality metrics, which measure nodal capability of functional integration (Bullmore and Bassett, 2011; Bullmore and Sporns, 2009; Rubinov and Sporns, 2010). Nodes with a high level of centrality, called hubs, are densely connected to a large number of other nodes (Achard et al., 2012; Achard et al., 2006; Zamora-López et al., 2010). Hubs are key to maintaining the functional topology of a human brain because they allow for efficient communication between regions (brain networking) independent of physical location (Bullmore and Sporns, 2009; Power et al., 2013). Hubs are prevalent in networks integrating multiple domains of cognitive and behavioral functioning, including default mode, fronto-parietal, salience, and sensorimotor networks (Buckner et al., 2009; Heuvel and Sporns, 2011; Power et al., 2013; Zamora-López et al., 2010). Deviation in hub topology, or hub disruption, is thought to be a reliable indicator of FC abnormalities associated with neurological disorder and insults (Achard et al., 2012; Crossley et al., 2014; Kaplan et al., 2019) and has been linked with individual differences in cognitive function (Cocuzza et al., 2020; Cohen and D'Esposito, 2016). Deviation in hub topology, whether due to centrality deficits in hubs or reorganization of nodal hubness, can be assessed with a newly developed metric, the hub disruption index (HDI), which quantifies nodal properties of the functional connectomes of clinical groups relative to those of healthy controls (Achard et al., 2012). For a given nodal graph metric, including centrality, the HDI is a fitted slope of the linear regression between the mean of the reference group and the difference between the clinical and reference groups. HDI is more influenced by deviations in nodes that are densely connected in the reference group. For these reasons, HDI is thought to be more sensitive to network topology changes compared to nodal centrality metrics (Achard et al., 2012; Termenon et al., 2016).

Graph theory research has documented hub-related changes and resulting topological re-organization in HIV disease (Abidin et al., 2018; Minosse et al., 2021; Minosse et al., 2020) and CU (de la Fuente et al., 2019; Konova et al., 2015; Liang et al., 2015) across widespread regions. Abidin et al. (2018) found an increase in hubs in the lateral occipital cortex, striatum, and thalamus in PWH relative to participants without HIV. Other studies have linked HIV disease with fewer hubs in the dorsal prefrontal cortex (PFC), cerebellum, somatosensory cortex, and left orbital PFC (Minosse et al., 2021; Minosse et al., 2020). Previous studies also showed HIV effects on topological deficits in executive functioning and default mode networks (Abidin et al., 2018; Minosse et al., 2020; Thomas et al., 2015), and we expect to observe HIV-related hub effects throughout multiple regions of these networks. Using HDIs, Minosse et al. (2020) found greater hub disruption of global degree, betweenness centrality (BC), efficiency, clustering coefficient, and spectral centrality in PWH compared to participants without HIV, but found fewer differences with nodal graph metrics. Although HDI has not been explored with CU, other research has suggested functional hub re-organization related to CU in multiple regions, including the striatum, default mode network, and salience network (de la Fuente et al., 2019; Konova et al., 2015; Liang et al., 2015). Based on these results, we expect to observe CU related hub effects in these networks.

The purpose of this study was to assess the independent and additive effects of HIV and CU on functional topology using metrics that describe network centrality and hubs. We measured hub disruption by quantifying the HDI for three centrality measures: BC, within module degree (WD), and participation coefficient (PC). Details for calculating these centrality metrics are described with equations in Section 2.5. BC was selected from other centrality metrics because it indicates both dense connections and short path lengths; both central properties of hubs (Bullmore and Sporns, 2009; Rubinov and Sporns, 2010). As a measure of network segregation, WD was chosen to measure the potential role of a node in network specialization of functioning. PC was chosen to provide information on each node's role in facilitating integration with other between networks. We expected to observe greater hub disruption in PWH and CU compared to controls. We also expected individuals with both HIV disease and CU to exhibit greater hub disruption compared to individuals with either condition alone. In contrast, we suspected that group differences in the nodal centrality metrics might not emerge as such metrics are less sensitive when not quantified as HDIs. Additionally, we expected greater hub disruption to be associated with lower scores on neurocognitive assessments and greater severity of HIV disease and CU.

2. Materials and methods

2.1. Participants and procedures

The study was open to adults aged 18–55 years with and without HIV who were stratified based on CU. Participants with HIV had a confirmed diagnosis of HIV disease for >3 months, while HIV-negative status was verified using an OraQuick© rapid test. CU was defined by the following criteria: regular CU for >1 year and either ≥2 days of use in the past 30 days or a cocaine-positive urine drug screen. Participants without CU met the following criteria: no lifetime cocaine dependence, no history of regular CU, no CU in the past 90 days, and a negative urine drug screen. Alcohol, nicotine, and marijuana use were allowed in all groups. For other substances, including amphetamine, heroin, and non-prescribed controlled medications (opioids and benzodiazepines or other sedatives), participants were excluded for: lifetime dependence, regular use for >2 years in the past 25 years, or regular use in the past 90 days. Additional exclusion criteria were: non-fluency in English; < 8th-grade education; severe learning disability; severe mental illness; current use of antipsychotic or mood-stabilizing medications; serious neurological disorders or history of neuroinfections; severe head trauma with loss of consciousness >30 minutes and persistent functional decline; and magnetic resonance imaging (MRI) contraindications. All participants

with HIV were currently treated with combined antiretroviral therapy (cART).

2.2. Measures

2.2.1. Clinical Data

Timeline Follow-Back methodology was used to asses substance use in the 30 days prior to the scan (Robinson et al., 2014; Sobell and Sobell, 1992), and the Addiction Severity Index – Lite (McLellan et al., 1992) was administered for lifetime use. The Structured Clinical Interview (Module E) for DSM-IV-TR was used to assess for current and past substance dependence (First et al., 2015). Participants completed an 11-panel urine toxicology screen and a breathalyzer. Using healthcare records, abstraction of HIV disease characteristics included most recent CD4 count, most recent viral load, years on cART, and duration of diagnosis.

2.2.2. Neuropsychological testing

Trained psychometrists administered a 45-minute battery to assess seven cognitive domains.

1. Processing Speed: Time (seconds) to complete Trail Making Test (TMT) Part A (Reitan and Wolfson, 1993); and number of color items completed on the Stroop Color and Word Test (Golden, 1978).
2. Learning: Total number of words recalled on trials 1–3 from the Hopkins-Verbal Learning Test- Revised (HVLT-R; Brandt and Benedict, 2001).
3. Memory: Total number of words recalled on trial 4 from the HVLT-R (Brandt and Benedict, 2001).
4. Executive functioning: Time (seconds) to complete TMT Part B (Reitan and Wolfson, 1993); and Stroop Color and Word Test (Golden, 1978) interference scores (difference between actual and predicted score on the color word trial).
5. Working Memory: Digit Span scores[1] from the NAB Digits Forward/Digits Backward Test (Stern and White, 2009) and Paced Auditory Serial Addition Task-50 (Diehr et al., 2003).
6. Verbal Fluency: Number of words generated in the Letter & Category Fluency Tests (Benton et al., 1983).
7. Motor function: Time (seconds) to complete the Grooved Pegboard Test (Klove, 1963) using each hand (yields scores for the dominant hand and non-dominant hand).

The test scores were converted to demographically corrected T-scores (M=50, SD=10) using up-to-date published norms (Diehr et al., 2003; Heaton et al., 2004; Stern and White, 2009; Wechsler, 2008). Each case was scored by two research assistants with a third research assistant resolving any discrepancies if needed. Test T-scores were averaged in each domain, yielding domain T-scores, which were averaged together to yield a global T-score.

2.2.3. MRI data acquisition

Participants abstained from drug use for at least four hours prior to their scans, except for nicotine to avoid withdrawal effects. A blood alcohol level of 0.00 was also required. Image acquisition was performed with a 3 T GE MR750 scanner with an eight-channel head coil at Duke University Hospital. While participants viewed a displayed cross-hair, Blood Oxygen Level Dependent (BOLD) functional MRI acquisition was done using T2*-weighted echo-planar imaging with the following parameters: repetition time (TR)= 2000 ms; echo time (TE)= 25 ms, in-plane matrix size= 64 ×64; slice thickness= 3.8 mm; field of view (FOV)= 24 cm, voxel size of 3.75 mm×3.75 mm×3.8 mm, flip angle=90°, 35 slices. Forty-nine participants differed: (TE=27 ms, flip angle=77°, 39 slices). For data harmonization, the first 150 volumes of each scan were included. Using a spoiled echo sequence, high-resolution T1-weighted (T1w) imaging acquisition involved the following parameters: TR = 8.16 ms, TE = 3.18 ms, voxel size = 1 mm x 1 mm x 1 mm, FOV = 256 mm^2, 256 * 256 matrix, 12° flip angle, 166 interleaved slice data acquisition.

2.3. MRI data preprocessing

2.3.1. Anatomical

The Brain Extraction Tool from fMRI Software Library (FSL) version 6.03 was used to remove anatomical matter outside the brain. Advanced Normalization Tools (ANTs) (v2.3.4; Avants et al., 2008) were used to calculate non-linear transformation matrices from T1w to Montreal Neurological Institute (MNI) - 152 standard space (2 mm^3).

2.3.2. Functional

The first six volumes of each functional scan were removed and 144 were retained. Motion Correction Functional Linear Registration Tool (MCFLIRT) from FSLv6.0.3 (Jenkinson et al., 2002) was used to calculate rigid body transformations matrices with six degrees of freedom (dof) and motion parameters. Two participants were excluded for having excessive motion (root mean square displacement >0.3 mm). Rigid body alignments from MCFLIRT were applied after slice timing correction with FSL Slicetimer. Functional to T1w affine transformation matrices (12 dof) were calculated using antsRegistrationSyN (Avants et al., 2008). Following mask dilation, voxels were normalized according to the median intensity value for each functional scan. Registration transformations matrices (previously calculated from ANTs) were applied to bring the functional data into standard MNI space. FAST algorithm from FSL (Smith et al., 2004) was used to calculate physiological noise regressors for subcortical white matter (WM) and cerebro-spinal fluid (CSF). Discrete Cosine-basis regressors (DCT) were calculated from the number of volumes and TR to exclude frequencies below 0.008 Hz. Functional data were then smoothed using a 6 mm gaussian Kernel. Non-aggressive denoising was performed using Automatic Removal of Motion Artifacts (AROMA) with the motion-correction parameters (Pruim et al., 2015). Afterwards, WM, CSF, and DCT were orthogonalized to the AROMA components, and a second regression was then performed to remove these confounds.

2.4. Construction of FC matrices

Using the Seitzman atlas (Seitzman et al., 2019), a 300 node atlas including subcortical regions based on the Power atlas (Power et al., 2011), we obtained the time-course of brain activity from each region across 144 time points. Regions with less than 75 % gray matter inclusion for at least one person were excluded from all analyses; 16 regions were excluded. We then computed correlations between all possible pairs of regions, creating a 284 ×284 correlation matrix. These correlation matrices were then fisher transformed. Correlations between nodes that were < 20 mm apart were not calculated, as close physical proximity may artificially inflate the correlation values (Power et al., 2012).

2.5. Graph metrics

2.5.1. Nodal graph metrics

Graph metrics were obtained using the brain connectivity toolbox (Rubinov and Sporns, 2010). The Louvain algorithm was used to define assignment into communities separately for each participant by maximizing modularity (Lancichinetti and Fortunato, 2012). The first step of this process involved generating optimal partitions 150 times (150

[1] For most participants, the NAB Digits Forward/Digits Backward Test (Stern and White, 2009) was adminsitered with both forward and backward digit spans converted to T-scores and then averaged. Some participants completed Wechsler Adult Intelligence Scale 4th Edition (Wechsler, 2008) Digit Span, and scores for those include forward, backward, and sequencing.

modular structures). A consensus partition was generated from 500 repetitions, and nodes had to be in same partitions at least 75 % of times to be counted (tau = 0.75). The matrices retained their edge weights and were thresholded in steps of 1 % from 1 % to 8 % density, as these thresholds yielded consistent degree distributions. Three nodal graph-theoretical metrics of centrality were calculated for each node across all modules (neural networks).

The betweenness centrality of a node is the proportion of shortest paths within the network on which the node falls.

$$BC_i = \frac{1}{(n-1)(n-2)} \sum_{\substack{h,j \in N \\ h \neq j, \\ h \neq i,}} \frac{p_{hj}(i)}{p_{hj}} \quad j \neq i \tag{1}$$

where p_{hj} is the number of shortest paths between nodes, h and j, and $p_{hj}(i)$ is the number of shortest paths that pass through i. The index of summation, h,j∈N, encompasses all paths between h and j that belong to the set of all nodes in network, N, where h, j, and i are distinct nodes. BC is calculated the same way for weighted matrices as for non-weighted matrices.

Within module degree is the sum of connection weights between a node and all other nodes within its module, m_i.

$$WD = k_i^w(m_i) \tag{2}$$

For analysis of nodal metrics, WD is standardized as a z-score relative to other nodes in the network.

$$z_i^w = \left(k_i^w(m_i) - k^w(m_i)\right) / \sigma^w(m_i) \tag{3}$$

$k^w(m_i)$ *and* $\sigma^w(m_i)$ are the mean and standard deviation of WD values for all nodes in module, m_i. A higher WD indicates greater local connectivity within a functional network. Greater network segregation is indicated by a higher WD and a lower PC.

Participation coefficient measures the diversity of modules to which a node is connected.

$$PC_i^w = 1 - \sum_{m \in M} \left(\frac{k_i^w(m)}{k_i^w}\right)^2 \tag{4}$$

Where M is the set of modules, and $k_i^w(m)$ is the weighted sum all of links between i and all nodes in module m. Note the summation index encompasses each module that is part of module set, M. A higher PC suggests greater integration between different functional networks.

2.5.2. HDI

The HDI is a global disruption index of any given nodal metric quantified in reference to a healthy control group (Achard et al., 2012). For each participant, a linear regression is performed on the metric of interest across all nodes, and the resulting beta value is the HDI. The average nodal metric value of each node of the control group constitutes the independent variable, and the difference between the control group average and the participant's nodal metric value at each node constitutes the dependent variable. The equation for this subject-wise regression is as follows for any given nodal metric, i (Minosse et al., 2019; Minosse et al., 2020).

$$NM_{i,l} - \frac{1}{C}\sum_{j=1}^{C} NM_{i,j} = k_{i,l}^0 + HDI_{i,l} * \frac{1}{C}\sum_{j=1}^{C} NM_{i,j} + \in_{i,l} \tag{5}$$

Where $NM_{i,l}$ is the network measure for all participants (l), $k_{i,l}^0$ is a constant term and $\in_{i,l}$ is the residual, and $\frac{1}{C}\sum_{j=1}^{C} NM_{i,j}$ represents the mean network measure for all control participants. An HDI is calculated for each node. When a participant's nodal values are similar to that of the control group, the HDI will be near zero. A negative HDI reflects a reduction in centrality relative to the control group. Greater hub disruption is suggested with larger negative values, which indicate reduced centrality in nodes that are highly central in the control group, and/or increased centrality in nodes that have low centrality in the control group (Achard et al., 2012). The three measures of centrality were quantified as HDIs (HDI-BC, HDI-WD, HDI-PC).

2.6. Analysis of group differences

Demographic data were compared using one-way ANOVAs and χ^2, as appropriate using SPSSv28.0. For nodal centrality metrics and HDI, the area under the curve (AUC) across 1–8 % density thresholds was calculated by integrating along the x-axis using the composite trapezoid rule. The AUCs were compared between groups using 2×2 ANCOVAs, controlling for education. Hub categorization was performed for each centrality metric with HDIs showing significant interactions. Nodes with average centrality in the 95th percentile for each group were classified as hubs. We compared if hubs in the HIV only, CU only, or HIV+CU groups differed from the controls.

2.7. Associations with cognitive functioning and disease characteristics

Across all participants, partial correlations were conducted between cognitive functioning and graph metrics. For PWH (HIV+CU and HIV only), partial correlations were conducted between HDIs and most recent CD4 count. For participants who use cocaine (HIV+CU and CU only), HDIs were correlated with years of regular use. We controlled for years of education in each of these analyses.

3. Results

3.1. Sample characteristics (Table 1)

There was a total of 206 participants (mean age = 44.4 years, 68 % male, 74 % African-American) categorized as follows: 41 PWH who use cocaine (HIV+CU), 36 CU only, 88 HIV only, and 41 controls. The groups did not differ in age, gender, or within scanner motion after processing. The groups with CU had a higher proportion of African American participants and lower levels of education compared to those without CU. Additionally, alcohol, cannabis, and daily cigarette use were more common in participants who used CU compared to those without CU. Global T-score was significantly higher among participants in the control group compared to the three other groups, as were T-scores for information processing, learning, memory, executive functioning, and motor domains (see supplementary table 2) (Table 1).

Most PWH (84.5 %) had a current undetectable viral load (VL < 50 count/uL). PWH reported an average duration of diagnosis of 12.9 years (SD=7.2), an average cART duration of 11.3 years (SD=7.6), and a median CD4 of 695 cells/uL (IQR = 2300). HIV disease characteristics did not differ by CU status.

Participants with CU averaged 10.8 days of use in the past month (SD = 8.8) and 16.5 years of regular use (SD = 8.7). There were no group differences in these CU characteristics by HIV status. Smoking was the predominant route of administration (81.8 %), which was more common in the CU only group compared to the HIV+CU group.

3.2. Centrality and hub disruption (Table 2, Fig. 1)

No significant differences for CU and/or HIV disease were found with the nodal centrality metrics, but significant differences between groups emerged when centrality metrics were quantified as HDIs. The pattern was similar for all three metrics, such that participants in the three clinical groups had larger negative HDI compared to the control group (Table 2, Fig. 1).

3.2.1. HDI-BC

There were main effects for both CU and HIV disease, suggesting greater BC hub disruption associated with each condition independently. Participants with CU had larger negative HDI-BC compared to

Table 1
Sample Characteristics.

	HIV+CU (N = 41)	CU only (N = 36)	HIV only (N = 88)	Control (N = 41)	Statistic	*p*-value
Age, M (SD)	44.9 (7.8)	45.4 (6.3)	44.6 (5.7)	42.8 (7.1)	F(3, 202) = 1.19	0.314
Gender, % male	72.7	66.7	71.6	58.5	$\chi^2(3) = 2.38$	0.498
Race, % Black (% White)	92.7 (4.9)	80.6 (13.9)	67.0 (29.5)	63.4 (29.3)	FET = 15.95	**0.008**
Years of education, M (SD)	12.8 (2.5)	12.6 (2.5)	14.12 (2.4)	14.5 (2.0)	F(3, 202) = 6.72	**<0.001**
Global T-score, M (SD)	44.5 (6.4)	44.5 (6.0)	45.2 (6.9)	50.2 (5.5)	F(3, 202) = 7.77	**<0.001**
fMRI motion, M (SD)*	0.019 (0.005)	0.020 (0.007)	0.017 (0.006)	0.019 (0.008)	F(3, 202) = 1.59	0.194
HIV disease characteristics						
Years on cART, M (SD)	11.2 (8.1)	N/A	11.3 (7.4)	N/A	t(127) = 0.11	0.91
Years diagnosed, M (SD)	12.1 (7.4)	N/A	13.3 (7.2)	N/A	t(127) = 0.87	0.386
Most recent CD4, median (IQR)	507 (588)	N/A	718 (496)	N/A	U(127) = 2287.50	**0.014**
Undetectable viral load (< 50), %	75.6	N/A	88.6	N/A	$\chi^2(1) = 3.62$	0.070
CU characteristics						
Years of regular use, M (SD)	15.7 (9.0)	17.5 (8.3)	N/A	N/A	t(75) = 0.90	0.369
Smoking admin, %	73.2	91.7	N/A	N/A	$\chi^2(1) = 4.41$	**0.043**
Days used in the past 30 days, M (SD)	10.9 (9.8)	10.6 (7.8)	N/A	N/A	F(3, 202) = 0.16	0.877
Other substance use						
Used alcohol in past 30 days, %	87.8	88.9	56.8	58.5	$\chi^2(3) = 21.61$	**<0.001**
Used cannabis in past 30 days, %	65.9	44.4	27.3	22.0	$\chi^2(3) = 23.08$	**<0.001**
Daily Cigarette Use, %	75.6	63.9	26.1	26.8	$\chi^2(3) = 38.84$	**<0.001**

* Root mean displacement

Table 2
Centrality metrics.

	HIV+CU (N = 41)	CU only (N = 36)	HIV only (N = 88)	Control (N = 41)	CU Main Effect	HIV Main Effect	CU x HIV
Betweenness Centrality							
HDI	−2.61 (0.33)	−2.29 (0.35)	−1.44 (0.22)	0.05 (0.33)	**F(1, 201) = 29.38, p < 0.001**	**F(1, 201) = 8.64, p = 0.004**	F(1, 201) = 3.52, p = 0.062
Unindexed	0.06 (0.00)	0.06 (0.00)	0.06 (0.00)	0.06 (0.00)	F(1, 201) = 0.33, p = 0.57	F(1, 201) = 0.02, p = 0.89	F(1, 201) = 0.82, p = 0.37
Participation Coefficient							
HDI	−2.85 (0.36)	−2.99 (0.39)	−2.24 (0.25)	0.03 (0.36)	**F(1, 201) = 25.66, p < 0.001**	**F(1, 201) = 9.82, p = 0.002**	**F(1, 201) = 12.35, p < 0.001**
Unindexed	1.48 (0.06)	1.44 (0.07)	1.43 (0.04)	1.44 (0.06)	F(1, 201) = 0.14, p = 0.71	F(1, 201) = 0.07, p = 0.79	F(1, 201) = 0.14, p=0.71
Within Module Degree							
HDI	−2.18 (0.33)	−2.17 (0.35)	−1.48 (0.22)	0.14 (0.33)	**F(1, 201) = 21.66, p = 0.001**	**F(1, 201) = 7.01, p = 0.009**	**F(1, 201) = 6.78, p = 0.010**
Unindexed*	45.54 (1.33)	47.26 (1.42)	45.65 (0.90)	45.63 (1.33)	F(1, 201) = 0.34, p = 0.56	F(1, 201) = 0.46, p = 0.50	F(1, 201) = 0.49, p = 0.49

Group analysis of both HDI and unindexed centrality metrics. Results from a 2 ×2 ANCOVA testing for the effects of HIV disease and CU while controlling for education are presented for each group as well as estimated marginal means (standard error). Partial correlations (controlling for years of education) between each centrality metric and cognitive functioning are presented in the last column. Bold values survived FDR corrections.
*Unstandardized within module degree.

participants without CU, and PWH had larger negative HDI compared to participants without HIV. However, there was no CU x HIV interaction for HDI-BC.

3.2.2. *HDI-WD*

There was a main effect for CU, a main effect for HIV disease, and a CU x HIV interaction. Among participants without CU, PWH (HIV only) had larger negative HDI-WD than controls. However, HIV had no effect among participants with CU, as HDI-WD did not differ between HIV+CU and CU only.

3.2.3. *HDI-PC*

There was a main effect for CU, a main effect for HIV disease, and a CU x HIV interaction. Among participants without CU, PWH had larger negative HDI-PC than participants without HIV (HIV only > controls). In contrast, HIV had no effect among participants with CU, as HDI-PC did not differ between HIV+CU and CU only.

3.2.4. *Description of WD hubs across groups (Fig. 2)*

The controls had WD hubs in the lateral occipital, dorsal prefrontal, and sensorimotor cortices, which were dispersed throughout fronto-parietal, default mode, and somatomotor networks. Compared to the controls, the CU only group had fewer WD hubs in the lateral occipital and dorsal prefrontal cortices, which belonged to the default mode, fronto-parietal, and visual networks. However, the CU only group had more sensorimotor hubs (somatomotor network) than the control group. Compared to the controls, the HIV only group also had fewer WD hubs in the lateral occipital (visual network) and dorsal prefrontal cortices (default mode and fronto-parietal networks), but had more WD hubs in the superior parietal lobule (somatomotor networks). Compared to the controls, the HIV+CU participants had fewer WD hubs in the lateral occipital and dorsal prefrontal cortices, indicating loss of hubs in default mode, visual, and fronto-parietal networks. However, HIV+CU participants had more sensorimotor hubs (Fig. 2).

3.2.5. *Description of PC hubs across groups (Fig. 3)*

The controls had PC hubs in the inferior frontal gyrus (ventral attention network), sensorimotor and paracingulate cortices (salience network), superior parietal and lateral occipital cortices (dorsal attention network), middle temporal gyrus (dorsal and ventral attention

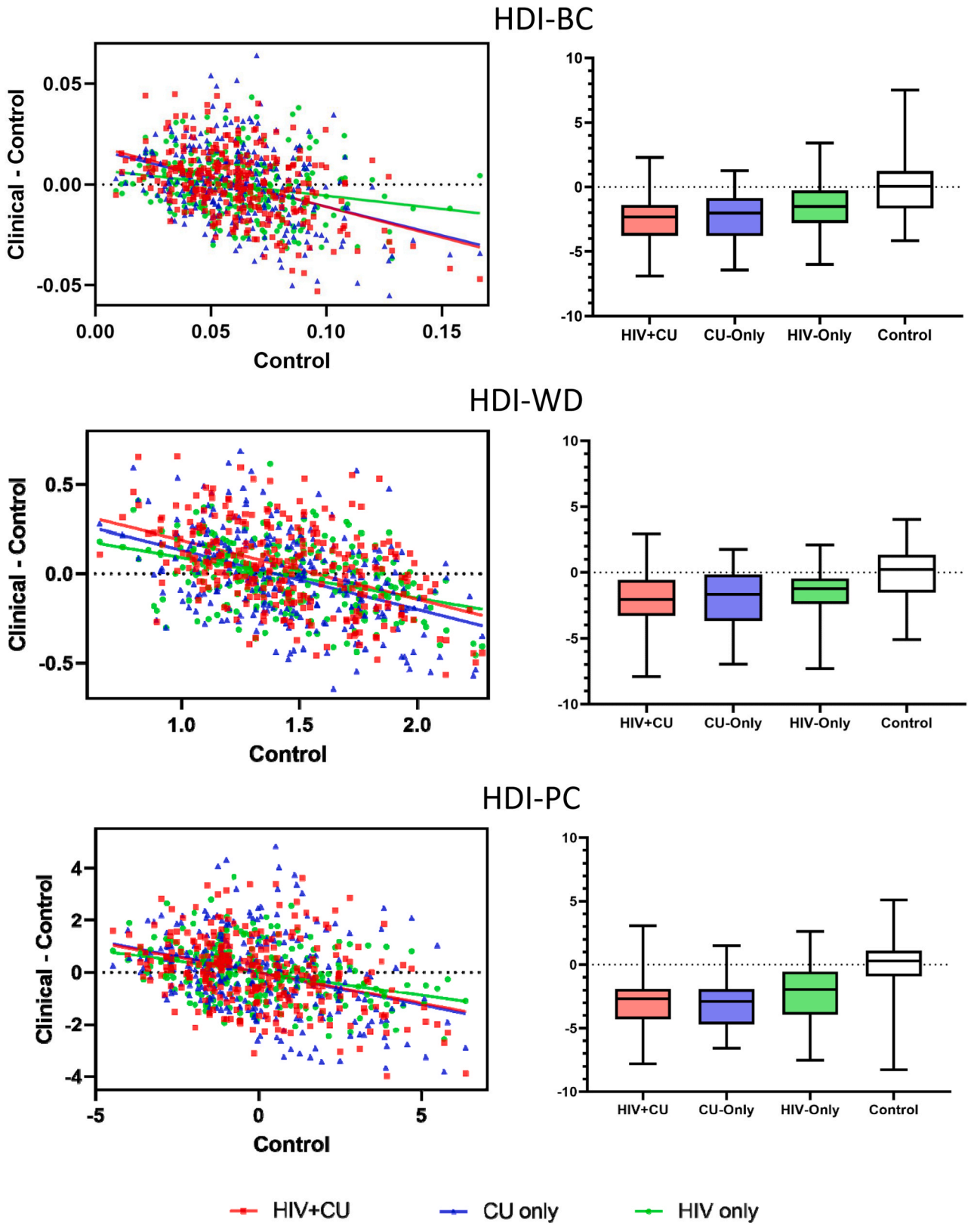

Fig. 1. Hub Disruption Index for each centrality metric. (Left) Plots of group HDIs (fitted slopes) using betweenness centrality (BC), within module degree (WD), and participation coefficient (PC) are displayed. Group-wise HDI using the following regression: $\frac{1}{H}\sum_{j=1}^{H} NM_{i,j} + \quad \frac{1}{C}\sum_{j=1}^{C} NM_{i,j} = k_i^0 + k_i * \quad \frac{1}{C}\sum_{j=1}^{C} NM_{i,j} + \quad \in_i$, Average nodal centrality metrics for the control group are plotted on the horizontal axes. Deviations scores between each clinical group and the control group are plotted on the vertical axes. (Right) Boxplots for HDI-BC, HDI-PC, and HDI-WD are displayed. All clinical groups (HIV+CU, HIV only, and CU only) show greater hub disruption (more negative HDI scores) compared to controls for all centrality measures.

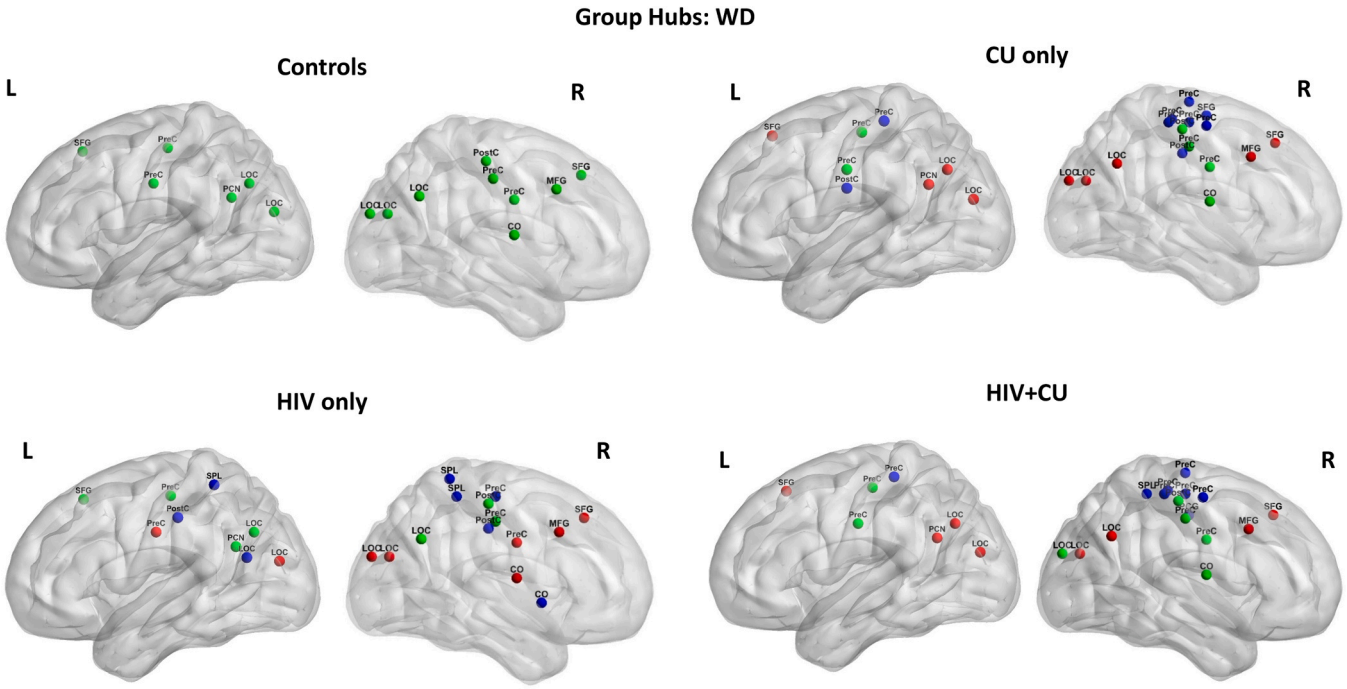

Fig. 2. Within module degree (WD) hubs for each group of participants. WD hubs are displayed in green for the control group (top left), and in each of the patient group relative to the controls. For the clinical groups (HIV only, CU only, HIV+CU), hubs are color coded in reference to the control group: Green – hub shared with controls; Red - hub is absent in clinical group, but present in control group; Blue – hub is present in clinical group only but not in control group. *Labels for brain regions.* SMA: Supplementary Motor Area, CO: Central Operculum, MTG: Middle Temporal Gyrus, LOC: Lateral Occipital Cortex, FP: Frontal Pole, IFG: Inferior Frontal Gyrus, MFG: Middle Frontal Gyrus, SPL: Superior Parietal Lobule, SMG: Supramarginal Gyrus, FO: Frontal Operculum, PCN: Precuneus, PreC: Precentral Gyrus; PostC: Postcentral Gyrus.

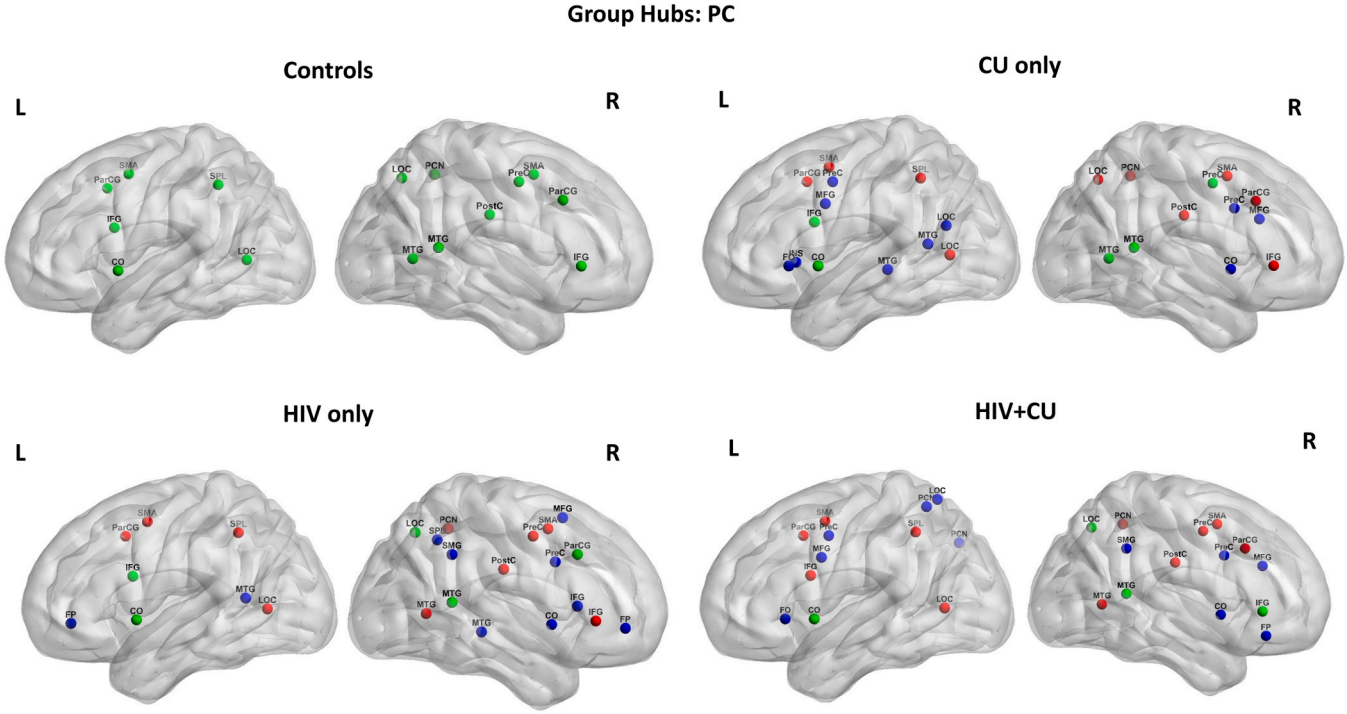

Fig. 3. Participation coefficient (PC) hubs for each group of participants. PC hubs are displayed in green for the control group (top left), and in each clinical group relative to the control group. For the clinical groups (HIV only, CU only, HIV+CU), hubs are color coded in reference to the control group: Green – hub shared with controls; Red - hub is absent in clinical group, but present in controls; Blue – hub is present in clinical group only but not in control group. *Labels for brain regions.* SMA: Supplementary Motor Area, CO: Central Operculum, MTG: Middle Temporal Gyrus, LOC: Lateral Occipital Cortex, FP: Frontal Pole, IFG: Inferior Frontal Gyrus, MFG: Middle Frontal Gyrus, SPL: Superior Parietal Lobule, SMG: Supramarginal Gyrus, FO: Frontal Operculum, PCN: Precuneus, PreC: Precentral Gyrus; PostC: Postcentral Gyrus.

networks), and in the supplementary motor regions from the cingulo-operculum network. Relative to the controls, the CU only group had fewer PC hubs in the paracingulate gyrus (salience network), and lateral parieto-occipital regions (dorsal attention network), but had more pre-frontal hubs (default, fronto-parietal, ventral attention networks). Relative to the controls, the HIV only group had fewer PC hubs in the precentral and supplementary motor gyri (cingulo-opercular network), and fewer lateral parieto-occipital hubs (dorsal attention network). However, the HIV only group had more right frontal PC hubs (fronto-parietal and ventral attention network) compared to the control group. Compared to the controls, the HIV+CU group also had fewer PC hubs in the paracingulate and supplementary motor cortex (salience network),

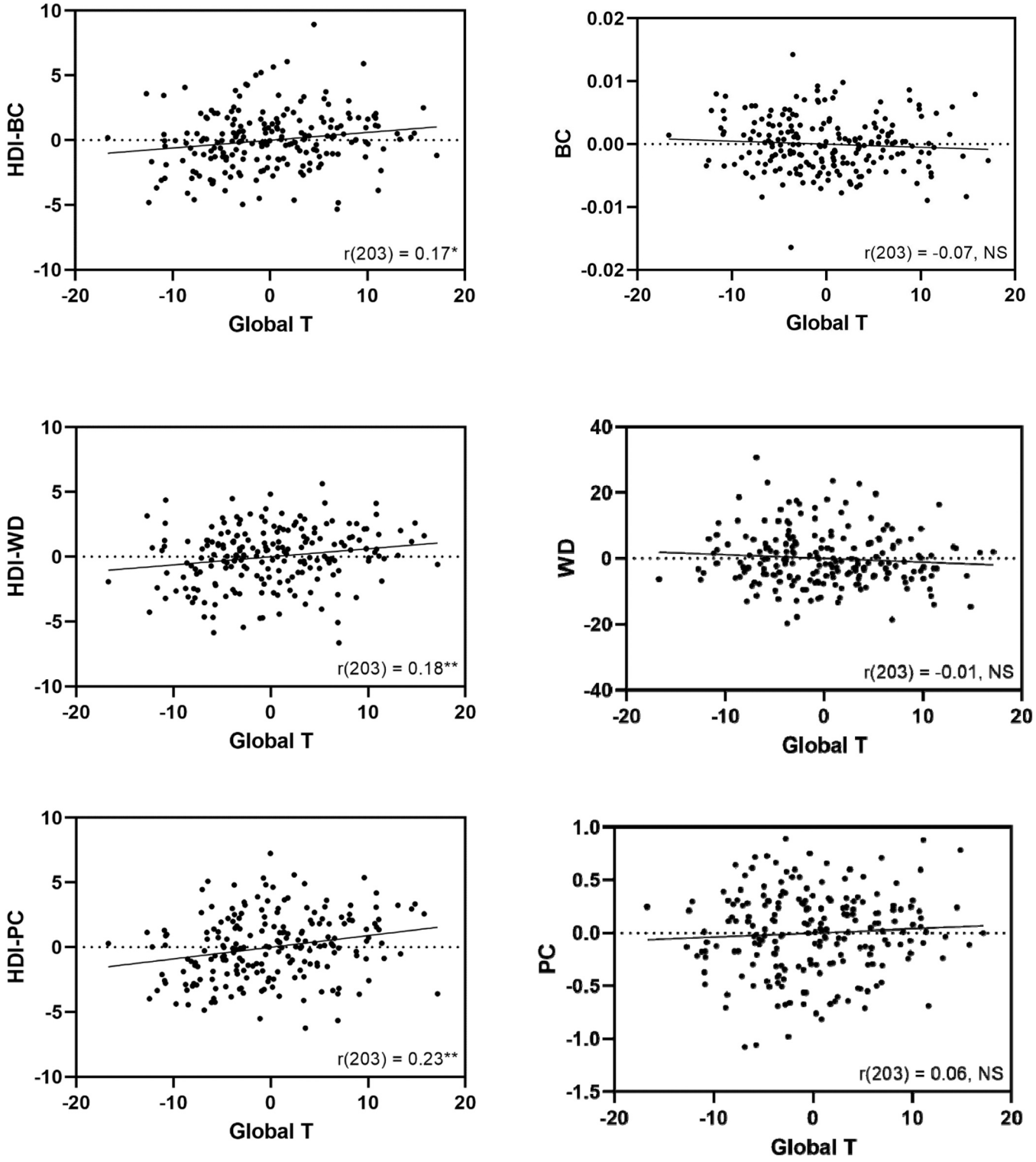

Fig. 4. Partial correlations between global T-scores and HDIs, controlling for years of education. (Left) Higher global T-scores (horizontal axes) are associated with lower hub disruption (more positive HDIs) for all centrality measures. (Right) Global T-scores were not associated with nodal centrality measures. *p<0.05, **p<0.01, NS: Not Significant.

lateral parieto-occipital cortices (dorsal attention network), and in the inferior frontal and middle temporal gyri (ventral attention network). However, HIV+CU had more PC hubs in the dorsal prefrontal cortex (fronto-parietal network) (Fig. 3).

3.3. Associations between centrality and cognitive functioning (Fig. 4)

Across all participants, larger negative HDIs were associated with lower Global T-scores (HDI-BC: r (203) = 0.17, $p < 0.05$ (FDR corrected, $p = 0.013$); HDI-PC: r(203) = 0.23, $p < 0.001$ (FDR corrected, $p = 0.002$); HDI-WD: r(203) = 0.18, $p < 0.01$ (FDR corrected, $p = 0.014$), suggesting that greater hub disruption is associated with lower cognitive functioning. In contrast, global T did not correlate with nodal centrality metrics (BC, PC, WD) (Fig. 4).

For domain T-scores (see supplementary table 3), lower information processing was associated with larger negative HDI-PC ($p < 0.001$) and HDI-WD ($p < 0.05$). Larger HDI-PC scores were also associated with lower attention ($p < 0.01$) and executive function scores ($p < 0.001$). Lower learning scores were associated with larger negative HDI-BC ($p < 0.05$). Memory and verbal fluency scores were not associated with HDI.

3.4. Associations between HDI and disease characteristic

For PWH, CD4 count was not associated with hub disruption (HDI-BC: r(125) = −0.02, p = 0.82; HDI-PC: r(125) = −0.05. p = 0.55; HDI-WD: r(125) = −0.09, p = 0.33). For participants with CU, hub disruption was not associated with years of regular use (HDI-BC: r(74) = −0.18, p = 0.12; HDI-PC: r(74) = −0.06. p = 0.62; HDI-WD: r(125) = −0.02, p = 0.87).

4. Discussion

Hub disruption was prominent in both persons with HIV disease and CU, with connectome deficits including betweenness centrality (i.e., nodal participation in shortest paths), within-module degree (i.e., within network connectivity/segregation of functional networks), and participation coefficient (i.e., between network integration). These findings suggest topological reorganization of functional neural networks resulting from deficits in multiple measures of hubness. In contrast, nodal graph metrics did not show differences between the healthy control group and persons with HIV disease and/or CU, underscoring the value of HDI as an index of brain functional reorganization. Our findings further supported the role of hubs in multiple aspects of cognitive functioning, including information processing and cognitive flexibility (Crossley et al., 2014; van den Heuvel and Sporns, 2013; Zuo et al., 2012), as hub-related functional network topology deficits were associated with lower cognitive functioning in these domains and globally. Our findings highlight disruption of functional hubs as potential biomarkers for HIV and cocaine-related neurocognitive function. Both PWH and persons with CU showed similar HDI effects, linking both conditions with deeply reorganized functional networks.

HIV disease was associated with greater hub disruption, but did not differ on nodal centrality measure from healthy controls. Consistent with previous research (Minosse et al., 2021; Minosse et al., 2020), our findings emphasize the role of hub reorganization in HIV-related FC deficits, further corroborating the sensitivity of HDI to disturbances in network topology. Here, we add to these findings by showing HIV effects on hub functioning related to centrality metrics associated with network integration and segregation. Widespread alterations of neural pathways is consistent with HIV neuropathology, which entails proliferation of infected macrophages, glial inflammation, and astrogliosis with consequential damage in multiple cortical and subcortical regions (Bell, 2004; Moore et al., 2006; Schouten et al., 2011). Specifically, glial cell dysfunction is linked to disruption of metabolic processes in neurons (Barros et al., 2018), which may be disproportionately damaging to hubs given their high metabolic demands (Crossley et al., 2014). Disturbances to the layout of neural networks can affect communication processes across the brain, which may be biomarker of HIV-related neurocognitive deficits.

To our knowledge, this is the first study using HDI to investigate CU effects on network centrality measures. Our findings expand on previous work showing FC density (Konova et al., 2015) and intermodule connectivity (Liang et al., 2015) deficits in CU by also documenting topological reorganization from disruption of centrality hubs. This is further supported by previously documented temporo-parietal shifted rich club organization, lower transitivity, and reduced striatal connectivity strength in persons with CU disorder (Hall et al., 2022). Hub-related topological effects in CU are consistent with neuroadaptations of dopaminergic circuitry within frontal and striatal neural regions evidenced in CU (Gowrishankar et al., 2014; Ma et al., 2015; Ma et al., 2015). Additionally, glial inflammation and astrocytosis have been observed in CU (Periyasamy et al., 2016), and resulting metabolic deficits in the central nervous system are thought to yield disproportionate effects on functional hubs (Crossley et al., 2014). Our findings of cocaine-related deficits in HDI, in conjunction with previously documented dopaminergic-modulated effects, implicate disruption of centrality hubs as a biomarker of neurocognitive deficits associated with CU. Moreover, centrality differences between participants with CU and healthy controls were undetectable by nodal metrics that do not particularly account for hub disruption.

Contrary to our hypothesis, analysis of HDIs did not show additive connectivity deficits, as hub disruption did not differ between the HIV+CU and HIV only, or between HIV+CU and CU only participants. CU and HIV effects were observed for HDI-WD and HDI-PC, but there was no additional effect of HIV among participants with CU and vice versa. The lack of additive effects likely results from limitation on how much disruption can occur with topological alterations, particularly in network segregation and integration. Prior task-based fMRI studies have documented additive deficits in FC and executive functioning in PWH who use cocaine (Bell et al., 2020; Meade et al., 2017; Wakim et al., 2022). Additive FC effects of CU and HIV may be more observable during tasks with high cognitive demands compared to resting state, as the former require extensive recruitment and modulation of cortical substrates. While the experimental designs of task-based fMRI studies provide more power to examine subtle changes in neural functioning in response to demands of varying intensity (e.g., increasing difficulty, risk, or salience), they are too complex to administer as part of standard clinical care.

We investigated PC and WD hub assignments within groups in order to further probe our interactive effects of HIV disease and CU on topological reorganization, and identified subtle changes in each of the clinical groups (HIV only, CU only, HIV+CU). Compared to controls, the clinical groups overall had fewer of the same PC hubs and more WD hubs in somato-motor and cingulo-operculum networks, linking both conditions with greater functional segregation in the networks. These observations suggest these regions are integral for functioning within their network instead of facilitating communication between distant regions of the brain in HIV disease and CU. However, the clinical groups overall also had more PC hubs and fewer WD hubs within the fronto-parietal, default mode, visual, ventral attention, and dorsal attention networks, which links both HIV disease and CU with disrupted functional specialization in these cortical networks. Indeed, decreased segregation of executive control and attention networks is consistent with top-down regulation of striatal reward processes in CU (Berlingeri et al., 2017; Feil et al., 2010; Hobkirk et al., 2019; Ma et al., 2015). Further, lower within network FC in the default mode, executive control, and dorsal attention networks have been linked to HIV Associated Neurocognitive Disorder (Chaganti et al., 2017; Thomas et al., 2015), and lower FC within default mode and salience networks have been observed in CU (Ding and Lee, 2013; Geng et al., 2017). Greater PC hubs in CU and HIV participants also suggests network topology disruption. Further, other research has found hyper-connectivity between functional cortical networks

contribute to executive functioning deficits in HIV disease (Lew et al., 2023). Mechanistically, between network connectivity disruptions involving the executive control, default mode, and salience networks underlie executive functioning deficits (Menon and Uddin, 2010), and such biomarkers are been linked to greater CU relapse (McHugh et al., 2017) and executive control deficits in HIV disease (Flannery et al., 2022). The shifting of hubs in HIV disease and CU, involving a mixture of increasing and decreasing centrality within multiple nodes, may help to explain the lack of group differences in nodal metrics. Other studies using stroke and comatose participants show nodal metrics to be less sensitive than HDI in detecting brain connectivity effects (Achard et al., 2012; Termenon et al., 2016). Further hub disruption has been found in many neurological diseases, including Alzheimer's disease, stroke, epilepsy, and amyotrophic lateral sclerosis (Daianu et al., 2016; Fornito et al., 2015; Grefkes and Fink, 2011; Menke et al., 2016; Pedersen et al., 2017; Ray et al., 2014).

Furthermore, we found associations between lower global cognitive functioning and greater hub disruption, but cognitive functioning did not correlate with the nodal metrics. Greater hub disruption was related to lower global cognitive functioning, highlighting the importance of healthy hub topology for better neuropsychological performance (Filippi et al., 2013; van den Heuvel and Sporns, 2013). Healthy cognitive function is predicated on a network organization structure with high centrality hub nodes that relay information across multiple edges simultaneously, and primarily reside in networks involved in integrated cognitive functioning, such as the default mode, fronto-parietal, salience, and sensorimotor networks (Buckner et al., 2009; Heuvel and Sporns, 2011; Sobell and Sobell, 1992; Zamora-López et al., 2010; Power et al., 2013). Alterations to organization of the functional connectome through reduced hub centrality can lead to poorer performance on cognitive tasks possibly due to disrupting integration of information between and within networks (Cocuzza et al., 2020; Cohen and D'Esposito, 2016; van den Heuvel and Sporns, 2019). The link between cognitive functioning to HDI, but not to nodal centrality metrics, supports the idea of increased sensitivity of HDI metrics in detecting cognitive impairment.

HDI was not associated with disease characteristics which may be partly attributed to limitations of these metrics as indicators of disease severity. As most of the HIV+CU and CU only groups had a history of chronic cocaine use, differences in years of use may not indicate variations in disease severity. Further, years of cocaine use was a self-report measure and subject to social desirability bias (Khalili et al., 2021; Latkin et al., 2017). Additionally, the most recent CD4 count may not reflect the duration of immunosuppression history in our participants with HIV as they have been treated with cART for many years. As such, we did not observe associations between HDI and CD4 count as were found in previous studies using a mixture of treated and untreated sample of participants with HIV (Minosse et al., 2021).

Strengths of this study include the 2-by-2 between-subjects design with a relatively robust sample size and the inclusion of a novel metric that provided greater sensitivity for detection of CU and HIV disease effects compared to nodal graph metrics. At the same time, the current study has some caveats. First, our resting state scans were relatively brief and some studies have suggested increasing test-retest reliability with longer scans (Birn et al., 2013). Additionally, the delineation of CU effects from other substance use is limited by poly-substance use collinearity; albeit we verified HDI differences between groups remained significant when adding alcohol, cannabis, and tobacco use as covariates to mitigate this limitation. Further, we implemented a cross-sectional design, which restricts our interpretations of HIV and cocaine-related hub disruptions to correlational inferences. Longitudinal research studies will allow for systematic analyses that differentiate HIV legacy effects from ongoing HIV neuropathogenesis. Additionally, future studies could examine HDI in CU from fMRI data collected during reward processing from monetary incentive tasks or visual cues with drug-laden stimuli to inform effects of dopaminergic signaling which is a potential avenue of inquiry consistent with top-down regulation deficits.

5. Conclusions

In sum, we found evidence of hub disruption independently associated with both HIV disease and CU, further supporting the importance of hubs in revealing information regarding functional network topology in brain disorders. The association between greater hub disruption and lower cognitive functioning in all centrality metrics reinforces the roles of hubs in cognitive processing that encompass neural networking characteristics of shortest path participation as well as integration and segregation of functional neural networks. Although HDI may have limitations with respect to location specificity, we show compelling evidence of bolsters HDI as a sensitive biomarker for topological effects. Focusing on hubs enabled detection of network abnormalities that were undetectable with nodal graph metrics.

Declarations ethics approval

All participants provided written informed consent for all study procedures. This study was approved by the institutional review board of the Duke University Health System.

Funding

This study was funded by grant # R01-DA045565 from the US National Institutes of Health. The NIH had no further role in the design of the study, data collection, data analysis, preparation, or the decision to submit the paper for publication.

CRediT authorship contribution statement

Shana A. Hall: Writing – review & editing, Writing – original draft, Software, Methodology, Formal analysis, Conceptualization. **James Mu:** Visualization, Software. **Syam Gadde:** Writing – review & editing, Validation, Software. **Jessica R. Cohen:** Writing – review & editing, Validation, Software, Methodology, Formal analysis, Conceptualization. **Sheri L. Towe:** Writing – review & editing, Supervision, Project administration, Data curation, Conceptualization. **Ryan P. Bell:** Writing – review & editing, Software, Formal analysis, Conceptualization. **Kareem Al-Khalil:** Writing – review & editing, Writing – original draft, Validation, Software, Methodology, Formal analysis, Conceptualization. **Christina S. Meade:** Writing – review & editing, Supervision, Methodology, Funding acquisition, Formal analysis, Conceptualization.

Declaration of Competing Interest

The authors declare no competing interests.

Appendix A. Supporting information

Supplementary data associated with this article can be found in the online version at doi:10.1016/j.drugalcdep.2024.112416.

References

Abidin, A.Z., DSouza, A.M., Nagarajan, M.B., Wang, L., Qiu, X., Schifitto, G., Wismuller, A., 2018. Alteration of brain network topology in HIV-associated neurocognitive disorder: a novel functional connectivity perspective. Neuroimage Clin. *17*, 768–777. https://doi.org/10.1016/j.nicl.2017.11.025.

Achard, S., Delon-Martin, C., Vertes, P.E., Renard, F., Schenck, M., Schneider, F., Bullmore, E.T., 2012. Hubs of brain functional networks are radically reorganized in comatose patients. Proc. Natl. Acad. Sci. USA *109* (50), 20608–20613. https://doi.org/10.1073/pnas.1208933109.

Achard, S., Salvador, R., Whitcher, B., Suckling, J., Bullmore, E., 2006. A resilient, low-frequency, small-world human brain functional network with highly connected association cortical hubs. J. Neurosci. *26* (1), 63–72. https://doi.org/10.1523/jneurosci.3874-05.2006.

Adinoff, B., Gu, H., Merrick, C., McHugh, M., Jeon-Slaughter, H., Lu, H., Stein, E.A., 2015. Basal hippocampal activity and its functional connectivity predicts cocaine relapse. Biol. Psychiatry *78* (7), 496–504. https://doi.org/10.1016/j.biopsych.2014.12.027.

Anand, P., Springer, S.A., Copenhaver, M.M., Altice, F.L., 2010. Neurocognitive impairment and HIV risk factors: a reciprocal relationship. AIDS Behav. *14* (6), 1213–1226. https://doi.org/10.1007/s10461-010-9684-1.

Ances, B.M., Ellis, R.J., 2007. Dementia and neurocognitive disorders due to HIV-1 infection. Semin Neurol. *27* (1), 86–92. https://doi.org/10.1055/s-2006-956759.

Avants, B.B., Epstein, C.L., Grossman, M., Gee, J.C., 2008. Symmetric diffeomorphic image registration with cross-correlation: evaluating automated labeling of elderly and neurodegenerative brain. Med Image Anal. *12* (1), 26–41. https://doi.org/10.1016/j.media.2007.06.004.

Barros, L.F., Brown, A., Swanson, R.A., 2018. Glia in brain energy metabolism: a perspective. Glia *66* (6), 1134–1137. https://doi.org/10.1002/glia.23316.

Bell, J.E., 2004. An update on the neuropathology of HIV in the HAART era. Histopathology *45* (6), 549–559. https://doi.org/10.1111/j.1365-2559.2004.02004.x.

Bell, R.P., Towe, S.L., Lalee, Z., Huettel, S.A., Meade, C.S., 2020. Neural sensitivity to risk in adults with co-occurring HIV infection and cocaine use disorder. Cogn. Affect Behav. Neurosci. *20* (4), 859–872. https://doi.org/10.3758/s13415-020-00806-4.

Benton, A., Hamsher, K., Sivan, A., 1983. Multilingual Aphasia Examination, 3rd ed. AJA Associates, Iowa City, IA.

Berlingeri, M., Losasso, D., Girolo, A., Cozzolino, E., Masullo, T., Scotto, M., Paulesu, E., 2017. Resting state brain connectivity patterns before eventual relapse into cocaine abuse. Behav. Brain Res *327*, 121–132. https://doi.org/10.1016/j.bbr.2017.01.002.

Birn, R.M., Molloy, E.K., Patriat, R., Parker, T., Meier, T.B., Kirk, G.R., Prabhakaran, V., 2013. The effect of scan length on the reliability of resting-state fMRI connectivity estimates. Neuroimage *83*, 550–558. https://doi.org/10.1016/j.neuroimage.2013.05.099.

Bowring, A., Maumet, C., Nichols, T.E., 2019. Exploring the impact of analysis software on task fMRI results. Hum. Brain Mapp. *40* (11), 3362–3384. https://doi.org/10.1002/hbm.24603.

Bowring, A., Nichols, T.E., Maumet, C., 2022. Isolating the sources of pipeline-variability in group-level task-fMRI results. Hum. Brain Mapp. *43* (3), 1112–1128. https://doi.org/10.1002/hbm.25713.

Brandt, J., & Benedict, R.H.B. (2001). Hopkins Verbal Learning Test – Revised Professional Manual. Lutz, FL: Psychological Assessment Resources, Inc.

Buckner, R.L., Sepulcre, J., Talukdar, T., Krienen, F.M., Liu, H., Hedden, T., Johnson, K. A., 2009. Cortical hubs revealed by intrinsic functional connectivity: mapping, assessment of stability, and relation to Alzheimer's disease. J. Neurosci. *29* (6), 1860–1873. https://doi.org/10.1523/jneurosci.5062-08.2009.

Bullmore, E.T., Bassett, D.S., 2011. Brain graphs: graphical models of the human brain connectome. Annu Rev. Clin. Psychol. *7*, 113–140. https://doi.org/10.1146/annurev-clinpsy-040510-143934.

Bullmore, E.T., Sporns, O., 2009. Complex brain networks: graph theoretical analysis of structural and functional systems. Nat. Rev. Neurosci. *10* (3), 186–198. https://doi.org/10.1038/nrn2575.

Cai, Y., Yang, L., Callen, S., Buch, S., 2016. Multiple Faceted Roles of Cocaine in Potentiation of HAND. Curr. HIV Res *14* (5), 412–416. https://doi.org/10.2174/1570162x14666160324125158.

Cattie, J.E., Doyle, K., Weber, E., Grant, I., Woods, S.P., 2012. Planning deficits in HIV-associated neurocognitive disorders: component processes, cognitive correlates, and implications for everyday functioning. J. Clin. Exp. Neuropsychol. *34* (9), 906–918. https://doi.org/10.1080/13803395.2012.692772.

Chaganti, J.R., Heinecke, A., Gates, T.M., Moffat, K.J., Brew, B.J., 2017. Functional connectivity in virally suppressed patients with HIV-associated neurocognitive disorder: a resting-state analysis. AJNR Am. J. Neuroradiol. *38* https://doi.org/10.3174/ajnr.A5246.

Chilunda, V., Calderon, T.M., Martinez-Aguado, P., Berman, J.W., 2019. The impact of substance abuse on HIV-mediated neuropathogenesis in the current ART era. Brain Res. *1724*, 146426 https://doi.org/10.1016/j.brainres.2019.146426.

Cisler, J.M., Elton, A., Kennedy, A.P., Young, J., Smitherman, S., Andrew James, G., Kilts, C.D., 2013. Altered functional connectivity of the insular cortex across prefrontal networks in cocaine addiction. Psychiatry Res. *213* (1), 39–46. https://doi.org/10.1016/j.pscychresns.2013.02.007.

Cocuzza, C.V., Ito, T., Schultz, D., Bassett, D.S., Cole, M.W., 2020. Flexible Coordinator and Switcher Hubs for Adaptive Task Control. J. Neurosci. *40* (36), 6949–6968. https://doi.org/10.1523/JNEUROSCI.2559-19.2020.

Cohen, J.R., D'Esposito, M., 2016. The Segregation and Integration of Distinct Brain Networks and Their Relationship to Cognition. J. Neurosci. *36* (48), 12083–12094. https://doi.org/10.1523/JNEUROSCI.2965-15.2016.

Crossley, N.A., Mechelli, A., Scott, J., Carletti, F., Fox, P.T., McGuire, P., Bullmore, E.T., 2014. The hubs of the human connectome are generally implicated in the anatomy of brain disorders. Brain *137* (Pt 8), 2382–2395. https://doi.org/10.1093/brain/awu132.

Cysique, L.A., Heaton, R.K., Kamminga, J., Lane, T., Gates, T.M., Moore, D.M., Brew, B. J., 2014. HIV-associated neurocognitive disorder in Australia: a case of a high-functioning and optimally treated cohort and implications for international neuroHIV research. J. Neurovirol *20* (3), 258–268. https://doi.org/10.1007/s13365-014-0242-x.

Cysique, L.A., Maruff, P., Brew, B.J., 2004. Prevalence and pattern of neuropsychological impairment in human immunodeficiency virus-infected/acquired immunodeficiency syndrome (HIV/AIDS) patients across pre- and post-highly active antiretroviral therapy eras: a combined study of two cohorts. J. Neurovirol *10* (6), 350–357. https://doi.org/10.1080/13550280490521078.

Daianu, M., Mezher, A., Mendez, M.F., Jahanshad, N., Jimenez, E.E., Thompson, P.M., 2016. Disrupted rich club network in behavioral variant frontotemporal dementia and early-onset Alzheimer's disease. Hum. Brain Mapp. *37* (3), 868–883. https://doi.org/10.1002/hbm.23069.

Diehr, M.C., Cherner, M., Wolfson, T.J., Miller, S.W., Grant, I., Heaton, R.K., 2003. The 50 and 100-item short forms of the Paced Auditory Serial Addition Task (PASAT): Demographically corrected norms and comparisons with the full PASAT in normal and clinical samples. J. Clin. Exp. Neuropsychol. *25* (4), 571–585. https://doi.org/10.1076/jcen.25.4.571.13876.

Ding, X., Lee, S.W., 2013. Cocaine addiction related reproducible brain regions of abnormal default-mode network functional connectivity: a group ICA study with different model orders. Neurosci. Lett. *548*, 110–114. https://doi.org/10.1016/j.neulet.2013.05.029.

du Plessis, S., Vink, M., Joska, J.A., Koutsilieri, E., Bagadia, A., Stein, D.J., Emsley, R., 2015. HIV infection is associated with impaired striatal function during inhibition with normal cortical functioning on functional MRI. J. Int Neuropsychol. Soc. *21* (9), 722–731. https://doi.org/10.1017/S1355617715000971.

Egbert, A.R., Biswal, B., Karunakaran, K., Gohel, S., Pluta, A., Wolak, T., Lojek, E., 2018. Age and HIV effects on resting state of the brain in relationship to neurocognitive functioning. Behav. Brain Res *344*, 20–27. https://doi.org/10.1016/j.bbr.2018.02.007.

Feil, J., Sheppard, D., Fitzgerald, P.B., Yucel, M., Lubman, D.I., Bradshaw, J.L., 2010. Addiction, compulsive drug seeking, and the role of frontostriatal mechanisms in regulating inhibitory control. Neurosci. Biobehav Rev. *35* (2), 248–275. https://doi.org/10.1016/j.neubiorev.2010.03.001.

Filippi, M., van den Heuvel, M.P., Fornito, A., He, Y., Hulshoff Pol, H.E., Agosta, F., Rocca, M.A., 2013. Assessment of system dysfunction in the brain through MRI-based connectomics. Lancet Neurol. *12* (12), 1189–1199. https://doi.org/10.1016/s1474-4422(13)70144-3.

First, M.B., Williams, J.B.W., Karg, R.S., & Spitzer, R.L. (2015). Structured Clinical Interview for DSM-5—Research Version (SCID-5 for DSM-5, Research Version; SCID-5-RV). Arlington, VA: American Psychiatric Association.

Flannery, J.S., Riedel, M.C., Hill-Bowen, L.D., Poudel, R., Bottenhorn, K.L., Salo, T., Sutherland, M.T., 2022. Altered large-scale brain network interactions associated with HIV infection and error processing. Netw. Neurosci. *6* (3), 791–815. https://doi.org/10.1162/netn_a_00241.

Fornito, A., Zalesky, A., Breakspear, M., 2015. The connectomics of brain disorders. Nat. Rev. Neurosci. *16* (3), 159–172. https://doi.org/10.1038/nrn3901.

de la Fuente, A., Sedeño, L., Vignaga, S.S., Ellmann, C., Sonzogni, S., Belluscio, L., Ibañez, A., 2019. Multimodal neurocognitive markers of interoceptive tuning in smoked cocaine. Neuropsychopharmacology *44* (8), 1425–1434. https://doi.org/10.1038/s41386-019-0370-3.

Geng, X., Hu, Y., Gu, H., Salmeron, B.J., Adinoff, B., Stein, E.A., Yang, Y., 2017. Salience and default mode network dysregulation in chronic cocaine users predict treatment outcome. Brain *140* (5), 1513–1524. https://doi.org/10.1093/brain/awx036.

Golden, C.J. (1978). Stroop Color and Word Test. Chicago, IL: Stoelting.

Gowrishankar, R., Hahn, M.K., Blakely, R.D., 2014. Good riddance to dopamine: roles for the dopamine transporter in synaptic function and dopamine-associated brain disorders. Neurochem Int *73*, 42–48. https://doi.org/10.1016/j.neuint.2013.10.016.

Grefkes, C., Fink, G.R., 2011. Reorganization of cerebral networks after stroke: new insights from neuroimaging with connectivity approaches. Brain *134* (Pt 5), 1264–1276. https://doi.org/10.1093/brain/awr033.

Hall, S.A., Bell, R.P., Gadde, S., Towe, S.L., Nadeem, M.T., McCann, P.S., Meade, C.S., 2022. Strengthened and posterior-shifted structural rich-club organization in people who use cocaine. Drug Alcohol Depend. *235*, 109436 https://doi.org/10.1016/j.drugalcdep.2022.109436.

Hall, S.A., Lalee, Z., Bell, R.P., Towe, S.L., Meade, C.S., 2021. Synergistic effects of HIV and marijuana use on functional brain network organization. Prog. Neuropsychopharmacol. Biol. Psychiatry *104*, 110040. https://doi.org/10.1016/j.pnpbp.2020.110040.

Heaton, R.K., Clifford, D.B., Franklin, D.R., Jr, Woods, S.P., Ake, C., Vaida, F., Group, C., 2010. HIV-associated neurocognitive disorders persist in the era of potent antiretroviral therapy: CHARTER Study. Neurology *75* (23), 2087–2096. https://doi.org/10.1212/WNL.0b013e318200d727.

Heaton, R.K., Marcotte, T.D., Mindt, M.R., Sadek, J., Moore, D.J., Bentley, H., Grant, I., 2004. The impact of HIV-associated neuropsychological impairment on everyday functioning. J. Int. Neuropsychol. Soc. *10* (3), 317–331. https://doi.org/10.1017/S1355617704102130.

Heuvel, M.P. v d, Sporns, O., 2011. Rich-club organization of the human connectome. J. Neurosci. 31 (44), 15775–15786 doi:10.1523/jneurosci.3539-11.2011.

Hobkirk, A.L., Bell, R.P., Utevsky, A.V., Huettel, S., Meade, C.S., 2019. Reward and executive control network resting-state functional connectivity is associated with impulsivity during reward-based decision making for cocaine users. Drug Alcohol Depend. *194*, 32–39. https://doi.org/10.1016/j.drugalcdep.2018.09.013.

Jenkinson, M., Bannister, P., Brady, M., Smith, S., 2002. Improved optimization for the robust and accurate linear registration and motion correction of brain images. Neuroimage *17* (2), 825–841. https://doi.org/10.1006/nimg.2002.1132.

Kaplan, C.M., Schrepf, A., Vatansever, D., Larkin, T.E., Mawla, I., Ichesco, E., Harris, R.E., 2019. Functional and neurochemical disruptions of brain hub topology in chronic pain. Pain *160* (4), 973–983. https://doi.org/10.1097/j.pain.0000000000001480.

Khalili, P., Nadimi, A.E., Baradaran, H.R., Janani, L., Rahimi-Movaghar, A., Rajabi, Z., Motevalian, S.A., 2021. Validity of self-reported substance use: research setting versus primary health care setting. Subst. Abus. Treat. Prev. Policy *16* (1), 66. https://doi.org/10.1186/s13011-021-00398-3.

Klove, H. (1963). Grooved Pegboard. Lafayette, IN: Lafayette Instruments.

Konova, A.B., Moeller, S.J., Tomasi, D., Goldstein, R.Z., 2015. Effects of chronic and acute stimulants on brain functional connectivity hubs. Brain Res *1628* (Pt A), 147–156. https://doi.org/10.1016/j.brainres.2015.02.002.

Lancichinetti, A., Fortunato, S., 2012. Consensus clustering in complex networks. Sci. Rep. *2*, 336. https://doi.org/10.1038/srep00336.

Latkin, C.A., Edwards, C., Davey-Rothwell, M.A., Tobin, K.E., 2017. The relationship between social desirability bias and self-reports of health, substance use, and social network factors among urban substance users in Baltimore, Maryland. Addict. Behav. *73*, 133–136. https://doi.org/10.1016/j.addbeh.2017.05.005.

Laverick, R., Haddow, L., Daskalopoulou, M., Lampe, F., Gilson, R., Speakman, A., Rodger, A., 2017. Self-reported decline in everyday function, cognitive symptoms, and cognitive function in people with HIV. J. Acquir. Immune Defic. Syndr. *76* (3), e74–e83. https://doi.org/10.1097/qai.0000000000001468.

Lew, B.J., McCusker, M.C., O'Neill, J., Bares, S.H., Wilson, T.W., Doucet, G.E., 2023. Resting state network connectivity alterations in HIV: Parallels with aging. Hum. Brain Mapp. *44* (13), 4679–4691. https://doi.org/10.1002/hbm.26409.

Li, Y., Cheng, P., Liang, L., Dong, H., Liu, H., Shen, W., Zhou, W., 2022. Abnormal resting-state functional connectome in methamphetamine-dependent patients and its application in machine-learning-based classification. Front Neurosci. *16*, 1014539 https://doi.org/10.3389/fnins.2022.1014539.

Li, X., Cong, J., Liu, K., Wang, P., Sun, M., Wei, B., 2023. Aberrant intrinsic functional brain topology in methamphetamine-dependent individuals after six-months of abstinence. Math. Biosci. Eng. *20* (11), 19565–19583. https://doi.org/10.3934/mbe.2023867.

Liang, X., He, Y., Salmeron, B.J., Gu, H., Stein, E.A., Yang, Y., 2015. Interactions between the salience and default-mode networks are disrupted in cocaine addiction. J. Neurosci. *35* (21), 8081–8090. https://doi.org/10.1523/JNEUROSCI.3188-14.2015.

Ma, L., Steinberg, J.L., Cunningham, K.A., Lane, S.D., Bjork, J.M., Neelakantan, H., Moeller, F.G., 2015. Inhibitory behavioral control: A stochastic dynamic causal modeling study comparing cocaine dependent subjects and controls. Neuroimage Clin. *7*, 837–847. https://doi.org/10.1016/j.nicl.2015.03.015.

Ma, L., Steinberg, J.L., Moeller, F.G., Johns, S.E., Narayana, P.A., 2015. Effect of cocaine dependence on brain connections: clinical implications. Expert Rev. Neurother. *15* (11), 1307–1319. https://doi.org/10.1586/14737175.2015.1103183.

Mansoory, M.S., Allahverdy, A., Behboudi, M., Khodamoradi, M., 2022. Local efficiency analysis of restingstate functional brain network in methamphetamine users. Behav. Brain Res. *434*, 114022 https://doi.org/10.1016/j.bbr.2022.114022.

McLellan, A.T., Kushner, H., Metzger, D., Peters, R., Smith, I., Grissom, G., Pettinati, H., Argeriou, M., 1992. The fifth edition of the addiction severity index. J. Subst. Abuse Treat. 9, 199–213. https://doi.org/10.1016/0740-5472(92)90062-s.

McHugh, M.J., Gu, H., Yang, Y., Adinoff, B., Stein, E.A., 2017. Executive control network connectivity strength protects against relapse to cocaine use. Addict. Biol. *22* (6), 1790–1801. https://doi.org/10.1111/adb.12448.

Meade, C.S., Hobkirk, A.L., Towe, S.L., Chen, N.K., Bell, R.P., Huettel, S.A., 2017. Cocaine dependence modulates the effect of HIV infection on brain activation during intertemporal decision making. Drug Alcohol Depend. *178*, 443–451. https://doi.org/10.1016/j.drugalcdep.2017.05.043.

Menke, R.A., Proudfoot, M., Wuu, J., Andersen, P.M., Talbot, K., Benatar, M., Turner, M. R., 2016. Increased functional connectivity common to symptomatic amyotrophic lateral sclerosis and those at genetic risk. J. Neurol. Neurosurg. Psychiatry *87* (6), 580–588. https://doi.org/10.1136/jnnp-2015-311945.

Menon, V., Uddin, L.Q., 2010. Saliency, switching, attention and control: a network model of insula function. Brain Struct. Funct. 214, 655–667. https://doi.org/10.1007/s00429-010-0262-0.

Minosse, S., Floris, R., Nucci, C., Toschi, N., Garaci, F., Martucci, A., Guerrisi, M., 2019. Disruption of brain network organization in primary open angle glaucoma. Annu Int Conf. IEEE Eng. Med Biol. Soc. *2019*, 4338–4341. https://doi.org/10.1109/embc.2019.8857290.

Minosse, S., Picchi, E., Di Giuliano, F., Sarmati, L., Teti, E., Pistolese, C.A., Garaci, F., 2021. Functional brain network reorganization in HIV infection. J. Neuroimaging *31* (4), 796–808. https://doi.org/10.1111/jon.12861.

Minosse, S., Picchi, E., Giuliano, F.D., Lanzafame, S., Manenti, G., Pistolese, C.A., Toschi, N., 2020. Disruption of brain network organization in patients with human immunodeficiency virus (HIV) infection. Annu Int Conf. IEEE Eng. Med Biol. Soc. *2020*, 1726–1729. https://doi.org/10.1109/embc44109.2020.9176449.

Moore, D.J., Masliah, E., Rippeth, J.D., Gonzalez, R., Carey, C.L., Cherner, M., Grant, I., 2006. Cortical and subcortical neurodegeneration is associated with HIV neurocognitive impairment. AIDS *20* (6), 879–887. https://doi.org/10.1097/01.aids.0000218552.69834.00.

Orsini, C.A., Colon-Perez, L.M., Heshmati, S.C., Setlow, B., Febo, M., 2018. Functional Connectivity of Chronic Cocaine Use Reveals Progressive Neuroadaptations in Neocortical, Striatal, and Limbic Networks. eNeuro *5* (4). https://doi.org/10.1523/eneuro.0081-18.2018.

Pedersen, M., Omidvarnia, A., Curwood, E.K., Walz, J.M., Rayner, G., Jackson, G.D., 2017. The dynamics of functional connectivity in neocortical focal epilepsy. Neuroimage Clin. *15*, 209–214. https://doi.org/10.1016/j.nicl.2017.04.005.

Periyasamy, P., Guo, M.L., Buch, S., 2016. Cocaine induces astrocytosis through ER stress-mediated activation of autophagy. Autophagy *12* (8), 1310–1329. https://doi.org/10.1080/15548627.2016.1183844.

Plessis, L., Paul, R.H., Hoare, J., Stein, D.J., Taylor, P.A., Meintjes, E.M., Joska, J.A., 2017. Resting-state functional magnetic resonance imaging in clade C HIV: within-group association with neurocognitive function. J. Neurovirol. *23* (6), 875–885. https://doi.org/10.1007/s13365-017-0581-5.

Power, J.D., Barnes, K.A., Snyder, A.Z., Schlaggar, B.L., Petersen, S.E., 2012. Spurious but systematic correlations in functional connectivity MRI networks arise from subject motion. NeuroImage *59* (3), 2142–2154. https://doi.org/10.1016/j.neuroimage.2011.10.018.

Power, J.D., Cohen, A.L., Nelson, S.M., Wig, G.S., Barnes, K.A., Church, J.A., Petersen, S. E., 2011. Functional network organization of the human brain. Neuron *72* (4), 665–678. https://doi.org/10.1016/j.neuron.2011.09.006.

Power, J.D., Schlaggar, B.L., Lessov-Schlaggar, C.N., Petersen, S.E., 2013. Evidence for hubs in human functional brain networks. Neuron *79* (4), 798–813. https://doi.org/10.1016/j.neuron.2013.07.035.

Pruim, R.H.R., Mennes, M., van Rooij, D., Llera, A., Buitelaar, J.K., Beckmann, C.F., 2015. ICA-AROMA: a robust ICA-based strategy for removing motion artifacts from fMRI data. Neuroimage *112*, 267–277. https://doi.org/10.1016/j.neuroimage.2015.02.064.

Ray, S., Miller, M., Karalunas, S., Robertson, C., Grayson, D.S., Cary, R.P., Fair, D.A., 2014. Structural and functional connectivity of the human brain in autism spectrum disorders and attention-deficit/hyperactivity disorder: a rich club-organization study. Hum. Brain Mapp. *35* (12), 6032–6048. https://doi.org/10.1002/hbm.22603.

Reitan, R.M., Wolfson, D., 1993. The Halstead-Reitan Neuropsychological Test Battery: Theory and Clinical Interpretation, 2nd ed. Neuropsycholgy Press, Tucson, AZ.

Robinson, S.M., Sobell, L.C., Sobell, M.B., Leo, G.I., 2014. Reliability of the Timeline Followback for cocaine, cannabis, and cigarette use. Psychol. Addict. Behav. *28* (1), 154–162. https://doi.org/10.1037/a0030992.

Rubinov, M., Sporns, O., 2010. Complex network measures of brain connectivity: uses and interpretations. Neuroimage *52* (3), 1059–1069. https://doi.org/10.1016/j.neuroimage.2009.10.003.

Sanmarti, M., Ibáñez, L., Huertas, S., Badenes, D., Dalmau, D., Slevin, M., Jaen, A., 2014. HIV-associated neurocognitive disorders. J. Mol. Psychiatry *2* (1), 2. https://doi.org/10.1186/2049-9256-2-2.

Schouten, J., Cinque, P., Gisslen, M., Reiss, P., Portegies, P., 2011. HIV-1 infection and cognitive impairment in the cART era: a review. AIDS *25* (5), 561–575. https://doi.org/10.1097/QAD.0b013e3283437f9a.

Seitzman, B.A., Gratton, C., Marek, S., Raut, R.V., Dosenbach, N.U.F., Schlaggar, B.L., Greene, D.J., 2019. A set of functionally-defined brain regions with improved representation of the subcortex and cerebellum. NeuroImage, 116290. https://doi.org/10.1016/j.neuroimage.2019.116290.

Shiau, S., Arpadi, S.M., Yin, M.T., Martins, S.S., 2017. Patterns of drug use and HIV infection among adults in a nationally representative sample. Addict. Behav. *68*, 39–44. https://doi.org/10.1016/j.addbeh.2017.01.015.

Shrestha, R., Copenhaver, M., 2016. The influence of neurocognitive impairment on HIV risk behaviors and intervention outcomes among high-risk substance users: a systematic review. Front. Public Health *4*, 1–6. https://doi.org/10.3389/fpubh.2016.00016.

Smith, S.M., Jenkinson, M., Woolrich, M.W., Beckmann, C.F., Behrens, T.E.J., Johansen-Berg, H., Bannister, P.R., De Luca, M., Drobnjak, I., Flitney, D.E., Niazy, R.K., Saunders, J., Vickers, J., Zhang, Y., De Stefano, N., Brady, J.M., Matthews, P.M., 2004. Advances in functional and structural MR image analysis and implementation as FSL. NeuroImage 23, S208–S219. https://doi.org/10.1016/j.neuroimage.2004.07.051.

Sobell, L., Sobell, M., 1992. Timeline follow-back. In: Allen, J.P. (Ed.), Measuring Alcohol Consumption: Psychosocial and Biochemical Methods. Humana Press, Totwa, NJ, pp. 41–72.

Sporns, O., 2018. Graph theory methods: applications in brain networks. Dialog-. Clin. Neurosci. *20* (2), 111–121. https://doi.org/10.31887/DCNS.2018.20.2/osporns.

Stern, R.A., White, T., 2009. NAB Digits Forward/Digits Backward Test: Professional Manual. Psychological Assessment Resources, Inc. (PAR), Lutz, FL.

Termenon, M., Achard, S., Jaillard, A., Delon-Martin, C., 2016. The "Hub Disruption Index," a reliable index sensitive to the brain networks reorganization. a study of the contralesional hemisphere in stroke. Front Comput. Neurosci. *10*, 84. https://doi.org/10.3389/fncom.2016.00084.

Thames, A.D., Arentoft, A., Rivera-Mindt, M., Hinkin, C.H., 2013. Functional disability in medication management and driving among individuals with HIV: a 1-year follow-up study. J. Clin. Exp. Neuropsychol. *35* (1), 49–58. https://doi.org/10.1080/13803395.2012.747596.

Thomas, J.B., Brier, M.R., Ortega, M., Benzinger, T.L., Ances, B.M., 2015. Weighted brain networks in disease: centrality and entropy in human immunodeficiency virus and aging. Neurobiol. Aging *36* (1), 401–412. https://doi.org/10.1016/j.neurobiolaging.2014.06.019.

van den Heuvel, M.P., Sporns, O., 2019. A cross-disorder connectome landscape of brain dysconnectivity. Nat. Rev. Neurosci. *20* (7), 435–446. https://doi.org/10.1038/s41583-019-0177-6.

van den Heuvel, M.P., Sporns, O., 2013. Network hubs in the human brain. Trends Cogn. Sci. *17* (12), 683–696. https://doi.org/10.1016/j.tics.2013.09.012.

Wakim, K.M., Freedman, E.G., Tivarus, M.E., Heinecke, A., Foxe, J.J., 2022. Assessing combinatorial effects of HIV infection and former cocaine dependence on cognitive control processes: a functional neuroimaging study of response inhibition. Neuropharmacology *203*, 108815. https://doi.org/10.1016/j.neuropharm.2021.108815.

Wang, X., Foryt, P., Ochs, R., Chung, J.H., Wu, Y., Parrish, T., Ragin, A.B., 2011. Abnormalities in resting-state functional connectivity in early human immunodeficiency virus infection. Brain Connect *1* (3), 207–217. https://doi.org/10.1089/brain.2011.0016.

Wang, Y., Liu, M., Lu, Q., Farrell, M., Lappin, J.M., Shi, J., Bao, Y., 2020. Global prevalence and burden of HIV-associated neurocognitive disorder: A meta-analysis. Neurology *95* (19), e2610–e2621. https://doi.org/10.1212/WNL.0000000000010752.

Wechsler, D., 2008. Wechsler Adult Intelligence Scale–Fourth Edition: Administration and Scoring Manual. Pearson, Bloomington, MN.

Wei, P., Bao, R., Fan, Y., 2022. Comparing the reliability of different ICA algorithms for fMRI analysis. PLoS One *17* (6), e0270556. https://doi.org/10.1371/journal.pone.0270556.

Zamora-López, G., Zhou, C., Kurths, J., 2010. Cortical hubs form a module for multisensory integration on top of the hierarchy of cortical networks. Front Neuroinform 4 (1). https://doi.org/10.3389/neuro.11.001.2010.

Zenebe, Y., Akele, B., Selassie, M., Necho, M., 2021. A systematic review and meta-analysis of HIV associated neurocognitive disorders (HAND) among people with HIV in Ethiopia. AIDS Res. Ther. *18* (1), 99. https://doi.org/10.1186/s12981-021-00424-1.

Zhuang, Y., Zhang, Z., Tivarus, M., Qiu, X., Zhong, J., Schifitto, G., 2021. Whole-brain computational modeling reveals disruption of microscale brain dynamics in HIV infected individuals. Hum. Brain Mapp. *42* (1), 95–109. https://doi.org/10.1002/hbm.25207.

Zuo, X.N., Ehmke, R., Mennes, M., Imperati, D., Castellanos, F.X., Sporns, O., Milham, M. P., 2012. Network centrality in the human functional connectome. Cereb. Cortex *22* (8), 1862–1875. https://doi.org/10.1093/cercor/bhr269.